Physics – Uspekhi **49** (3) 263 – 273 (2006)

PHYSICS OF OUR DAYS

PACS numbers: **12.38. – t**, **12.39. – x**, 13.66.Bc, **13.87. – a**

Quantum chromodynamics and phenomenology of strong interactions

I M Dremin, A B Kaidalov

DOI: 10.1070/PU2006v049n03ABEH005873

Contents

Abstract. A brief survey of the strong interaction theory is presented. The basic principles of quantum chromodynamics and phenomenological approaches to strong interaction processes are described. Their predictions and recent achievements in describing experimental data at high energies are considered.

1. Introduction

Strongly interacting particles (hadrons) are the constituents of visible matter in nature with a typical scale of masses about 1 GeV. The forces for other particles (leptons, neutrinos, photons) are not so strong because they participate only in electroweak and gravitational interactions. This helps in calculating characteristics of their interactions using the perturbative approach once the interaction Lagrangian is known. There is no such simple remedy for hadrons. Nevertheless, it happens that the perturbation theory can also be applied in quantum chromodynamics to some special processes of strong interactions at high energies. Even in these cases, however, one has to use some additional assumptions and phenomenological constructions to describe experimental data.

I M Dremin Lebedev Physics Institute, Russian Academy of Sciences, 119991 Moscow, Leninskii prosp. 53, Russian Federation
Tel. (7-495) 132 29 29
E-mail: dremin@td.lpi.ru
A B Kaidalov Russian Federation State Scientific Center "Alikhanov Institute for Theoretical and Experimental Physics," ul. B. Cheremushkinskaya 25, 117218 Moscow, Russian Federation
Tel. (7-495) 129 94 31
E-mail: kaidalov@mail.itep.ru

Received 25 August 2005, revised 10 October 2005
Uspekhi Fizicheskikh Nauk **176** (2) 275 – 287 (2006)
Translated by I M Dremin, A B Kaidalov;
edited by A M Semikhatov

In this paper, we review all these problems. The paper is based on a plenary talk given by the authors at the conference on theoretical physics "TD70" devoted to the 70th anniversary of the Tamm Department of Theoretical Physics of the Lebedev Physical Institute of the Russian Academy of Sciences held in Moscow in April 2005. The talk was aimed at highly qualified physicists not working directly in the field of high-energy physics but interested in recent achievements in this field. Therefore, besides presenting a rather complete picture during very short time, it was necessary to describe it in an intelligible manner. The scope of the review is very wide, and to explore it in a simple but complete way, we have to restrict ourselves to particle production at high energies and omit static properties of strongly interacting particles (hadrons) and processes at low energy, as well as many technical details. That is why at the end of this broad survey of physics of our days, we refer the reader to only some textbooks and published review papers, where details dealing with particular problems are presented. Further references to the original papers (in particular, to experimental data and their theoretical fits, shown in the figures) can be found in these reviews as well as in recent publications and websites.

We do not describe the history of experimental studies and stages in our theoretical understanding of strong interactions. However, it is instructive to recall the very first steps in the discoveries of strong interacting particles.

The proton was the only known strongly interacting particle before Chadwick discovered the neutron in 1932. The same year, Heisenberg and Ivanenko independently published papers in which they claimed that atomic nuclei consist of protons and neutrons. The electromagnetic and gravitational forces known at that time could not explain the fact that protons and neutrons are bound inside nuclei. The forces were too long-range and weak to produce this effect at nuclear sizes. The neutron is somewhat heavier than the proton. In the free state, it decays into a proton, electron, and neutrino. In 1934, Fermi proposed the theory of this decay with new weak forces that were extremely short-range.

This inspired Tamm the same year [1] to suppose that these forces could govern proton – neutron interactions inside nuclei because they should be short-range, as can be easily guessed from the dimension of the Fermi coupling constant. He abandoned this attempt because the forces were too weak. Nevertheless, the idea that protons and neutrons should exchange via a massive object (the electron – neutrino pair is massive!) was accepted by Yukawa, who was brave enough to propose in 1935 that the exchanged object is a new, still unknown strongly interacting particle — the pion. Since then, pions have been discovered in cosmic rays, and it was understood that they are abundantly produced in strong interactions of hadrons and nuclei at high energies.

Intensive theoretical work on the problems of multiparticle production at high energies due to strong interactions began in the 1950s, when the statistical and hydrodynamical models of central interactions and the one-pion exchange model of peripheral interactions were proposed. The new class of inelastic diffraction processes was also considered. Nowadays, the main theoretical framework is provided by quantum chromodynamics (QCD) as a theory of strong interactions of hadrons, which are considered mediated by the color interactions of quarks and gluons. The yet unsolved problems of color confinement, however, force us to use simplified models at some stages. Numerous analytic and computer calculations and many Monte Carlo simulations using QCD ideas and approaches (often embedded within definite models) have been done in attempts to describe experimental data on the e^+e-, ep-, $pp(\bar{p}p)$-, pA-, AA-interactions at high energies and have proved to be very successful.

2. QCD Lagrangian

The main breakthrough in theory applications to high-energy processes began after the Lagrangian of quantum chromodynamics was written,

$$L = \mathrm{i}\sum_q \bar{\psi}_q^a(\nabla_\mu\gamma_\mu + \mathrm{i}m_q)\,\psi_q^a - \frac{1}{4}\,G_{\mu\nu}^n G_{\mu\nu}^n\,, \tag{1}$$

where

$$\nabla_\mu = \partial_\mu - \mathrm{i}g\,\frac{\lambda^n}{2}\,A_\mu^n\,, \tag{2}$$

$$G_{\mu\nu}^n = \partial_\mu A_\nu^n - \partial_\nu A_\mu^n + g f^{nml} A_\mu^m A_\nu^l\,. \tag{3}$$

Here, ψ_q^a and A_μ^n are quark and gluon fields, $a = 1, 2, 3$, and n, m, $l = 1, 2, \ldots, 8$ are color indices, λ^n and f^{nml} are the Gell-Mann matrices and f-symbols, m_q are bare (current) quark masses, and the index $q = \mathrm{u}, \mathrm{d}, \mathrm{s}, \mathrm{c}, \mathrm{b}, \mathrm{t}$ denotes quark flavors.

Lagrangian (1) contains both free-propagation and interaction terms of quarks and gluons with the coupling strength determined by g.

2.1 Asymptotic freedom

Especially important for practical purposes is the so-called asymptotic freedom property of the processes described by Lagrangian (1). According to it, the coupling strength of the interactions between quarks and gluons decreases at high energy scale p (the quark masses can be neglected). In the first-order approximation, it can be written at large p as

$$\alpha_\mathrm{s} = \frac{g^2}{4\pi} = \frac{6\pi}{(33 - 2n_\mathrm{f})\ln(p/p_0)}\,, \tag{4}$$

where n_f is the number of active flavors q and $p_0 = \mathrm{const}$ is the QCD scale parameter, which is of the order of hundreds of MeV. The higher approximations for α_s are often used with this parameter denoted as Λ_QCD, but it is sometimes simpler to apply formula (4) with p_0 as an adjustable parameter that accounts phenomenologically for the higher-order corrections and should be close to Λ_QCD.

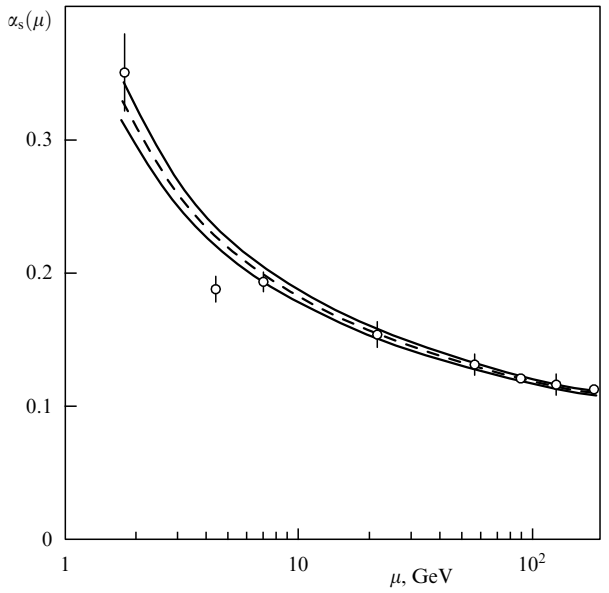

Figure 1. The QCD coupling strength decreases at high energy scales.

This decrease in the coupling strength with the energy scale has been confirmed in experiment, see Fig. 1. This decrease is directly related to the self-coupling of gluons described by the nonlinear terms in the Lagrangian. It shows that color forces become less powerful at short distances. This property of asymptotic freedom allows applying the whole machinery of the perturbation theory in considering high-energy processes and multiparticle production in particular.

2.2 Confinement

Even though the QCD Lagrangian has very impressive features, its eigenstates are quarks and gluons, whose free states are not directly observable. Hadrons observable in experiment are not eigenstates of QCD. QCD should explain this remarkable feature. However, no final solution to the confinement problem yet exists. Some additional assumptions are necessary at both low and high energies.

In the low-energy domain, the coupling strength becomes large and the perturbative approach is inapplicable. One has to rely on estimates coming from nonperturbative methods. One of them is proposed by lattice calculations. Other methods are related to the sum rules and studies of correlators.

Several other phenomenological approaches (such as the bag model) have also been proposed. In most of them, the crucial ingredient is the notion of quark – gluon condensates, corresponding to the nontrivial structure of the QCD vacuum, which is still not well understood. Phenomenologi-

[1] Just at the very end of 1934, I E Tamm founded the Department of Theoretical Physics in the Lebedev Physical Institute and became its head.

cally, hadrons can be described as confined states of the constituent quarks. Therefore, the potential models are quite successful in predicting the properties of quarkonia.

2.3 Soft hadronization

High-energy reactions are usually described as an evolution of systems of quarks and gluons. At the initial stage, one should consider hadrons as bunches of quarks and gluons and introduce the phenomenological structure (or fragmentation) functions. At the final stage of the quark – gluon cascade, one should also deal with the phenomenology of transformation of quarks and gluons into hadrons. One of the successful assumptions used here is the so-called local parton – hadron duality (LPHD) hypothesis. It declares that the inclusive characteristics of the quark – gluon shower remain valid for hadron distributions up to some constant energy-independent factor. This implies a soft hadronization stage for all multiparticle reactions. Another way is to introduce the phenomenological parton fragmentation functions.

3. e^+e^- annihilation

We start describing QCD applications to particular processes with the e^+e^- annihilation because it has the simplest initial state. In high-energy electron – positron collisions, the electron and positron convert into a virtual photon (or Z^0 boson), which produces a quark – antiquark pair as shown in Fig. 2. As we discuss below, each member of this pair reveals itself in experiment as a hadronic jet (schematically shown in Fig. 3). Its formation is described in QCD as a two-stage process.

In accordance with the QCD Lagrangian, each high-energy quark (or antiquark) can emit gluons, which in turn emit new gluons or quark – antiquark pairs. Thus the quark – gluon shower is produced. This stage is completely controlled by the perturbative QCD until the energies of partons (quarks and gluons) become very low, and partons are converted into hadrons.

The last stage is manifestly nonperturbative. Here, the hypothesis about the local parton – hadron duality is used to say that the calculated inclusive characteristics of partons are not crucially changed by the hadronization, and can also be used for hadrons. Symbolically, both stages are represented by the diagram in Fig. 4. Accepting this LPHD hypothesis, one can compare experimental data for hadrons with theoretically derived properties of parton showers. It turns out that such a hypothesis works quite well for inclusive characteristics.

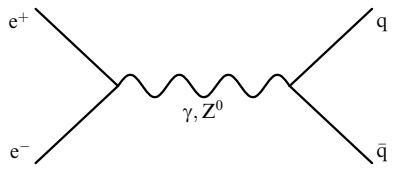

Figure 2. Feynman graph of e^+e^- annihilation in a quark – antiquark pair.

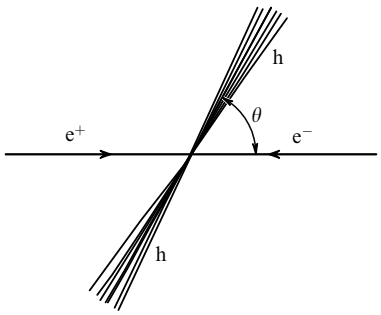

Figure 3. The process of annihilation of an electron – positron pair in two hadronic jets.

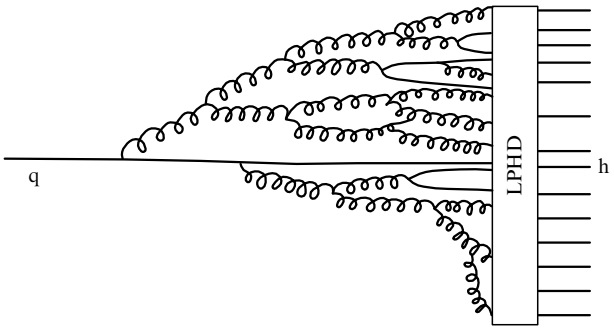

Figure 4. Evolution of a quark jet with the partonic stage and hadronization included.

3.1 Early days

To be trusted, the picture described above had to be proved in the early days when the very first results on e^+e^- annihilation were obtained. The primary question was whether one really observes two jets belonging to the created quark and antiquark.

3.1.1 Jets. It has been found that there is no isotropy in this process. The angular distribution of hadrons is pencil-like. It is schematically demonstrated in Fig. 3 by two jets moving in opposite directions. The partons in Fig. 2 actually determine the axes of these jets and their angular distribution, as discussed in more detail below. Many characteristics were used to demonstrate the jet-like structure of individual events. They were called sphericity, spherocity, thrust, etc. We do not go into the details of analysis but just conclude that the jet-like structure of the process has been firmly established. The directions of the jet axes were quite well determined by the criteria imposed according to the above characteristics. It is important that the Feynman graph in Fig. 2 also predicted that these jets should be initiated by partons having spin 1/2, and this had to be proved by experiment as well.

3.1.2 Spin. The distribution of quark directions in processes described by Fig. 2 is easily calculated and is given by the expression specific for the emission of partons with spin 1/2 at the angle θ to the e^+e^- collision axis:

$$\frac{d\sigma}{d\theta} \propto 1 + \cos^2\theta\,. \tag{5}$$

Because the jet axis was identified with the parton direction, θ is also the angle between the jet axis and the collision direction. Both of them are measured in experiment, and distribution (5) fitted the data very well. Moreover, QCD predicted that jets should remember the electric charges of the partons initiating them.

3.1.3 Quarks. Quarks are partons with noninteger electric charges e_q. The probability of creating a definite quark – antiquark pair according to Fig. 2 should be proportional

to e_q^2. The number of such pairs must be proportional to the number of colors, 3, with which quarks can be produced and the number of effective flavors playing a role at a definite energy of the e^+e^- collision. Its ratio to the probability of creating a $\mu^+\mu^-$ -pair with charges ± 1 is given by

$$R = \frac{\sigma_{\rm tot}^{e^+e^-\to h}}{\sigma^{e^+e^-\to\mu^+\mu^-}} = 3\sum_{q=1}^{n_f} e_q^2 . \tag{6}$$

The word 'effective' refers to the fact that quarks of different flavors have different masses.

Heavy quarks cannot be produced at low energies. Therefore, the number of effective quarks n_f up to which the summation range extends in (6) increases with energy. This gives rise to some threshold behavior in the energy dependence of R. Both the absolute value of R and its energy behavior predicted by QCD have been confirmed by experiment. This has provided a firm background to our belief in the applicability of QCD to the description of multiparticle production in e^+e^- annihilation.

3.2 Jet studies

After quark jets were firmly established as ingredients of multiparticle production processes, the problem of the theoretical description of their internal structure became especially crucial. This sector e^+e^- annihilation, they evolve decreasing their time-like virtuality by the emission of gluons and new quark–antiquark pairs. In turn, gluons develop gluon jets. The system of two integro-differential equations, the so-called DGLAP equations, was proposed for describing the evolution of quark and gluon jets.

3.2.1 DGLAP equations. In principle, for theoretical purposes, one can study the gluon sector of QCD only, without referring to quarks. This sector is called gluodynamics. It is self-contained and its predictions are qualitatively valid for the more general case. The understanding of the general picture becomes more transparent, and we therefore begin with describing gluodynamics. The system of two equations is replaced by a single equation, which can be written symbolically as

$$\text{EVOLUTION} = \text{INFLOW} - \text{OUTFLOW}$$

or

$$G' = \int \mathrm{d}\Omega\, \alpha_s K \left[G \otimes G - G\right] . \tag{7}$$

The evolution is determined by the derivative of the generating functional G of the inclusive characteristics of the considered process $G' \equiv \mathrm{d}G/\mathrm{d}y$ with respect to the logarithm of the energy $y = \ln p/p_0$ of massless partons. The kernel (weight) $\alpha_s K$ is determined by the QCD Lagrangian. The integration is over the available phase space Ω. The first term in the brackets corresponds to the fission of a gluon into two gluons. The second term describes the disappearance of a gluon from the phase space Ω due to fusion. Thus, Eqn (7) demonstrates the QCD kinetics of the process.

In the general case, as mentioned above, one obtains a system of two nonlinear integro-differential equations for quarks and gluons. This system can be solved by perturbative expansion in the powers of the coupling strength α_s. The specifics of this expansion in QCD is the running property of the coupling strength, i.e., its dependence on energy. Moreover, because the kernel K also depends on the energy shared by the partons, its different terms contribute differently to approximations of the various orders. The energy conservation at the fission process also has to be taken into account in the perturbative expansion. That is why this method is often called the 'modified perturbation theory.' The solutions of QCD equations in higher-order perturbative approximations improve agreement with experiment at presently available energies. Asymptotically, the results of the lowest-order approximation should be valid. However, this asymptotic domain lies far away, as follows from comparison with experimental data. We note that these equations can be solved exactly if one assumes that the coupling strength is fixed, i.e., does not depend on energy.

3.3 QCD predictions and their comparison with experiment

3.3.1 Multiplicities. The most general characteristic of multiparticle production processes is the multiplicity distribution. It shows the probability of creating a definite number of particles in a given process at some energy. As any probability distribution, it can also be described by its mean and higher-rank moments. The system of equations for them has been obtained from the equations for generating functions (7). It is crucial for QCD or for any phenomenological model to provide the proper multiplicity distribution because other inclusive characteristics are usually obtained by averaging over it. Any model that fails to properly describe multiplicity distribution cannot claim validity by fitting other inclusive distributions.

a. *Energy dependence of mean values*. The solution of the equations for the average multiplicities $\bar{n}$ in the lowest-order perturbative approximation has led to the prediction of a quite specific energy increase of mean multiplicities like

$$\bar{n} \propto \exp\left[c\,(\ln s)^{1/2}\right], \quad s = E_{\rm c.m}^2 . \tag{8}$$

The constant c is uniquely determined by the QCD Lagrangian. We note that this dependence is intermediate between the logarithmic ones, typical for peripheral processes or the Feynman plateau, $\bar{n} \propto \ln s$, and power-law dependences typical for fixed-coupling QCD or hydrodynamics, $\bar{n} \propto s^{1/4}$.

Some additional more slowly varying factors appear in higher-order solutions. The experimental data are well-fitted by QCD predictions, as shown in Fig. 5. Moreover, the slope and curvature of this dependence have been calculated and coincide well with experiment. They are differently sensitive to higher-order terms and therefore provide additional tests of the validity of their calculation within QCD.

b. *Ratio of mean multiplicities in gluon and quark jets*. A more important role is played by higher-order perturbative corrections to the ratio of mean multiplicities in gluon and quark jets, r. In the lowest-order approximation, it was predicted to stay constantly independent of the energy and to be equal to the ratio of Casimir operators for gluon and quark jets:

$$r_0 = \frac{C_V}{C_F} = 2.25; \tag{9}$$

In other words, gluon jets are much more active in producing secondary partons. In experiment, this ratio is close to 1.5 at the Z^0 resonance and even smaller at lower energies. In theory, however, this ratio continues to keep the same value

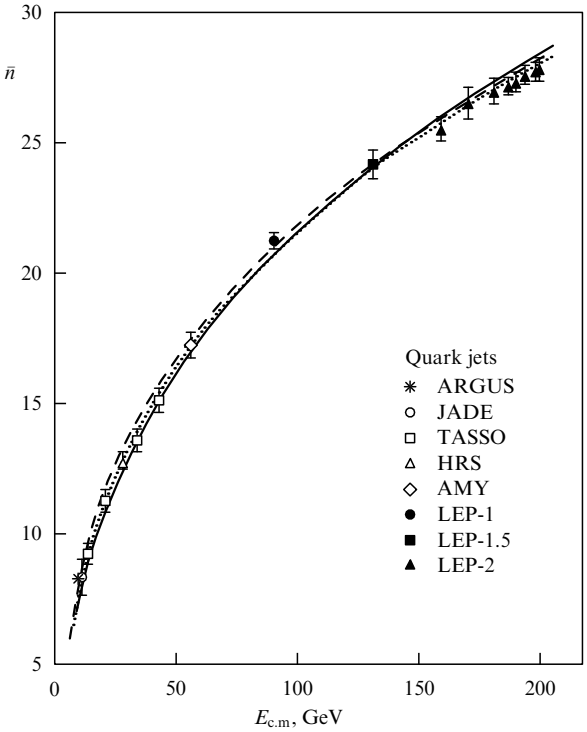

Figure 5. The mean charged particle multiplicity of e^+e^- hadronic annihilation events versus the energy scale $Q = E_{c.m.}$. The one- and two-parameter fits by QCD expressions fit the data well.

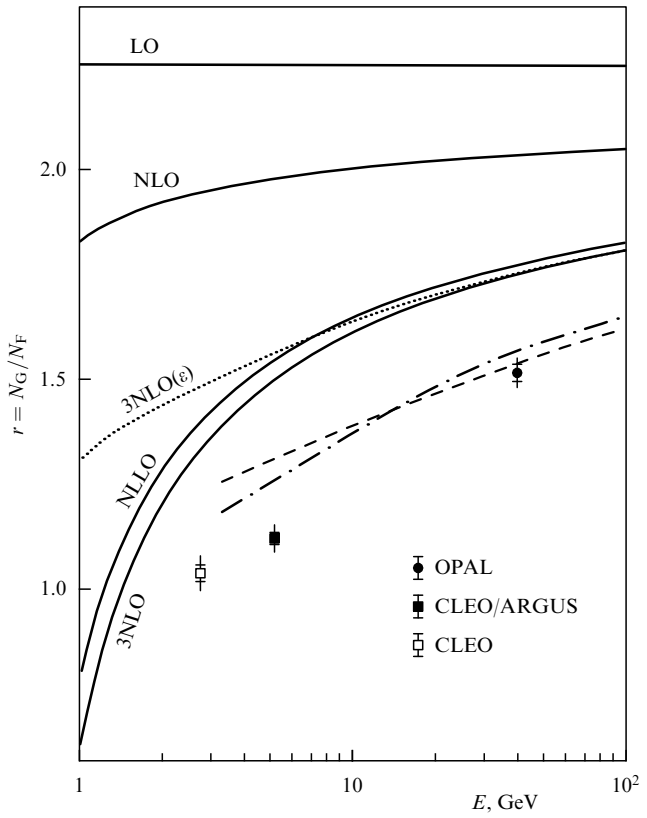

Figure 6. Experimental results for the multiplicity ratio of gluon and quark jets in comparison with the QCD analytic predictions (solid lines) and the HERWIG Monte Carlo model (dashed lines).

2.25 even in the next-to-leading approximation because the energy dependences of average multiplicities for gluon and quark jets stay the same up to this constant factor. Only in higher orders does one obtain theoretical analytic values closer to the experimental ones. The small difference left is avoided in Monte Carlo models by considering some contribution from the hadronization stage. Thus, good agreement with experiment is achieved, as demonstrated in Fig. 6. The exact computer solution of QCD equations provides a very good fit to experimental data even at the Υ resonance with hadronization taken into account in accordance with the LPHD hypothesis.

The approach to the asymptotic limit is very slow in Fig. 6. The theoretical values of r increase at higher energies because of the asymptotic freedom property of the coupling strength. One can try to mimic the asymptotic conditions by selecting only soft particles inside jets such that the conservation laws become less important. This has been done and has shown that the measured value of r for soft particles is 1.8 at the Z^0 resonance energy. It is larger than for all particles, but demonstrates that larger values of the coupling strength for soft partons and hadronization effects still prevent us from obtaining the asymptotic value of r for soft particles. It has been confirmed that in accordance with QCD predictions, r increases to 2.25 at the parton level if the hadronization effects are taken into account in accordance with the HERWIG model.

c. *Shapes of multiplicity distributions.* The shape of the multiplicity distribution P_n determines its moments. Traditionally, the well-known moments such as dispersion, kurtosity, etc. are used. In particular, it has been shown that dispersions of multiplicity distributions for gluon jets are larger than those for quark jets, i.e., gluon jets are more widely distributed in multiplicities. At the same time, the use of the so-called factorial and cumulant moments has become more customary. The factorial moments are defined as

$$F_q = \sum_{n=0}^{\infty} n\,(n-1)\ldots(n-q+1)\,P_n\,. \qquad (10)$$

They show the deviation from the Poisson distribution (for which they are identically equal to one). They can be represented as the derivatives of the generating function that helps obtain QCD equations for them from (7). Correspondingly, the cumulant moments K_q are calculated as the derivatives of the logarithm of the generating function. For the Poisson distribution, they are equal to zero, except for the first moment, which is equal to one. While the factorial moment of the qth order contains all correlations of the q-particle system, the cumulant moments describe the genuine correlations between those q particles that are irreducible to subsets of lower-order correlations, which indicates the absence of independent subgroups in the q-particle system. For those acquainted with quantum field theory, this is reminiscent of the complete set of Feynman graphs and their subset that does not contain the disconnected graphs. Both factorial and cumulant moments rapidly increase with their rank q. Therefore, for practical purposes, it is more convenient to use their ratio $H_q = K_q/F_q$, which is most easily calculated in the lowest-order QCD approximation. All these moments are equivalent in the sense that they can be expressed through each other by certain algebraic recursive relations.

Factorial moments, considered as functions of their rank q, are always positive by definition (10). QCD predicts that the cumulant and H_q moments are also positive when

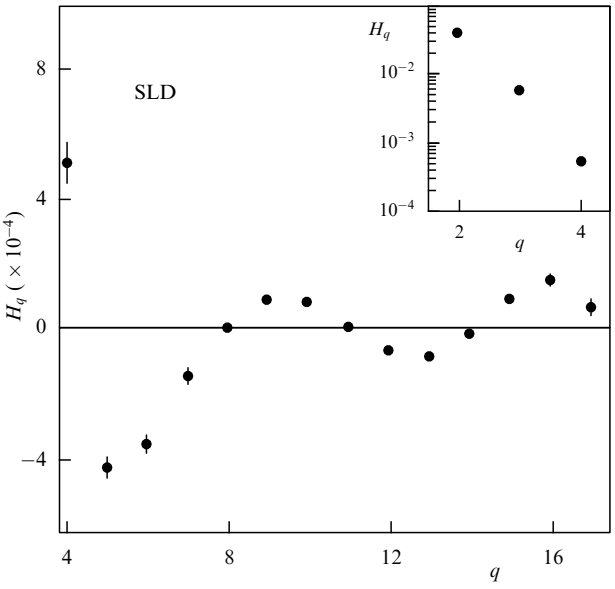

Figure 7. The measured ratio of cumulant to factorial moments H_q, as a function of the rank q, for the charged particle multiplicity distribution in e^+e^- hadronic Z^0 decays.

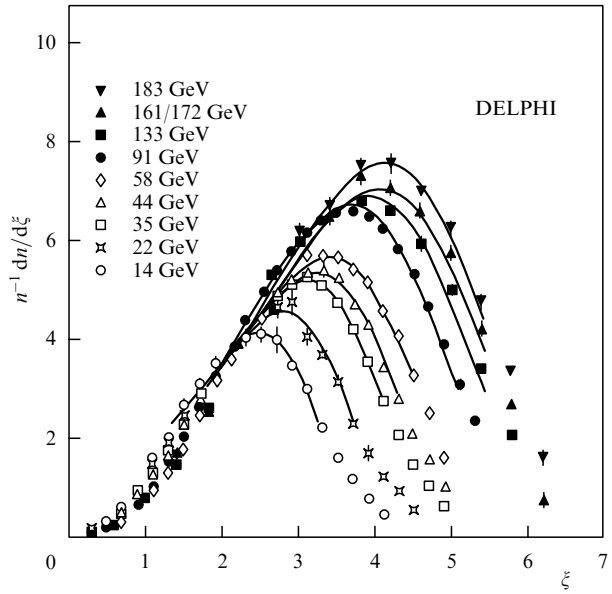

Figure 8. The peak in the particle distribution versus ξ in the e^+e^- annihilation, described by the slightly modified Gaussian shape and shifts to larger ξ at higher energies.

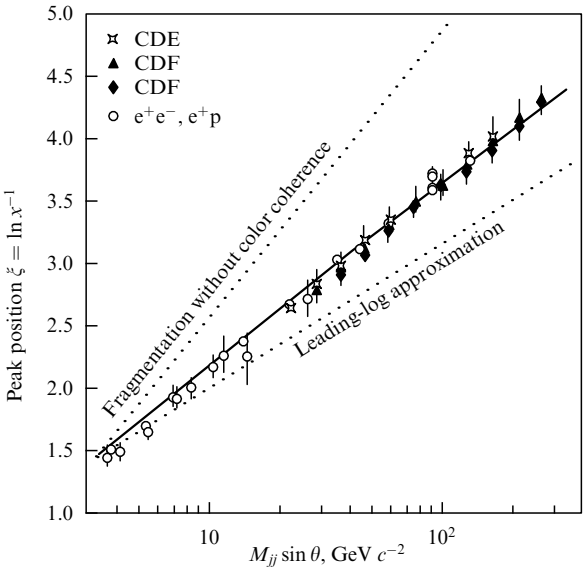

Figure 9. The peak position is well described by the next-to-leading order QCD (solid line) at all energies in e^+e^-, ep, $p\bar{p}$ reactions.

calculated in the lowest-order approximation, where the answer is especially simple: $H_q \sim 1/q^2$. Such behavior should reveal itself at asymptotically high energies. However, if calculated in higher orders, i.e., at finite energies, they become negative at a quite definite and predictable value of the rank q and start oscillating as the rank increases. At present energies, the first minimum should be placed at $q = 5$. Exact computer solutions of the equations lead to the same conclusions. This specific feature of the cumulant moments and, in particular, the predicted location of the first minimum has been confirmed by various experimental data, for example, by that in Fig. 7.

The distributions used in the probability theory do not usually have such a property. It can be validated for their combinations only. Even more important could be the analogy with statistical physics, where cumulant moments play the role of virial coefficients. The changing sign of virial coefficients sometimes indicates the properties such as superfluidity and superconductivity. This analogy has not yet been exploited in QCD.

3.3.2 Hump-backed plateau. The solution of the QCD equations for the generating functionals predicts a quite special shape of the distribution of the share (x) of the jet energy devoted to a single parton. It should have the form of a hump-backed plateau, as opposed to the flat plateau predicted by the Feynman parton model. The dip between the two humps appears due to the angular ordering and color coherence effects. It is necessary to consider the mutual screening of color charges moving close to each other. The 'color transparency' of such pairs is another effect induced by this screening. [2]

In the logarithmic scale $\xi = \ln x^{-1}$, the humps have an almost Gaussian form. The positions of their maxima move to larger values of ξ with an increase in energy approximately logarithmically. These predictions have been confirmed by experiment, as seen in Figs 8 and 9, where only one hump is shown due to the symmetry of their positions on the x axis. It is especially interesting that similar peaks and their energy dependence have been found in ep and $p\bar{p}$ processes. According to Fig. 9, they have the same regularities as in e^+e^- annihilation.

3.3.3 Phase-space structure: subjets, intermittency, fractality. Phase-space positions and multiplicities of particles in individual events fluctuate. These fluctuations become larger in smaller phase-space bins. At relatively low transferred momenta, the jet evolves into angular (or p_t) ordered subjets. More and more subjets are observed as the angular resolution is increased. The subjet multiplicities have been

[2] This has an analogue in electrodynamic processes, where it is called the Chudakov effect.

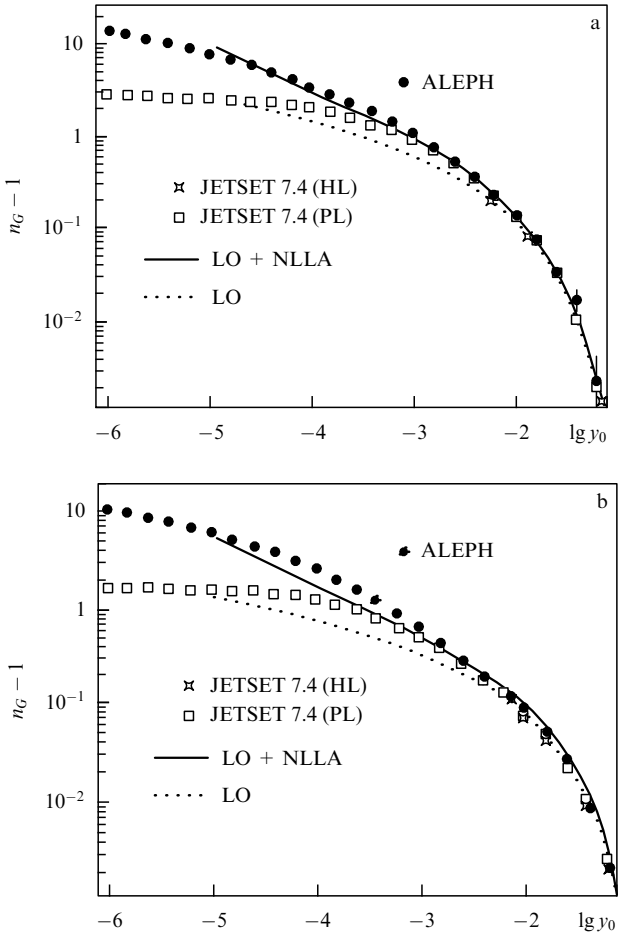

Figure 10. The subjet multiplicities of gluon (a) and quark (b) jets in comparison with analytic results (leading order LO, next approximation LO + NLLA), and Monte Carlo predictions (Jetset).

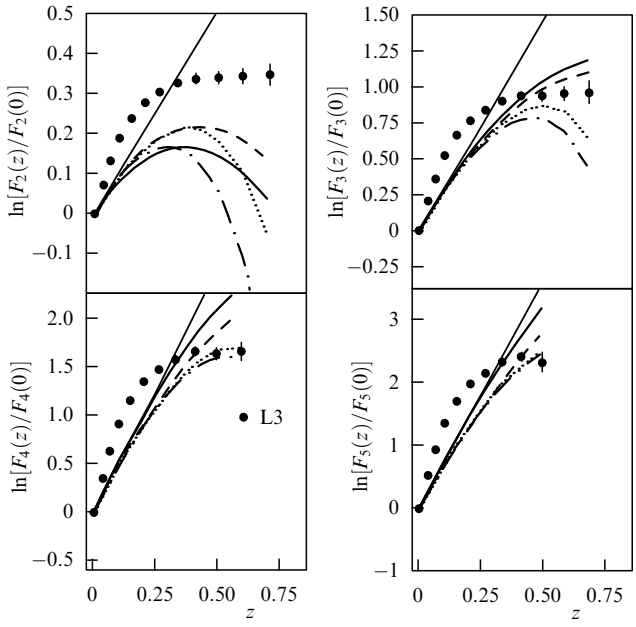

Figure 11. In the double-logarithmic scale, the ratios $F_q(z)/F_q(0)$ increase almost linearly at small z (monofractal) and flatten out at larger z (multifractal) in qualitative agreement with QCD predictions with the running coupling strength.

studied both experimentally and theoretically. Good agreement has been found as seen in Fig. 10.

This structure of individual events with the approximate self-similarity of subjets inside the jets leads to the remarkable property of intermittency and fractality, reminiscent of turbulence with selfsimilar whorls. This should correspond to a power-law increase of the factorial moments with decreasing the size of the phase-space bin for which this moment is calculated. For small angular intervals $\delta\theta$, they should obey the law

$$F_q \propto (\delta\theta)^{-\phi(q)} \tag{11}$$

with positive intermittency indices $\phi(q)$. This demonstrates the increase in fluctuations in smaller bins.

QCD predicts a linear increase of factorial moments in the double-logarithmic scale at comparatively large bins and their flattening for smaller bins due to the running property of the coupling strength. This is clearly demonstrated in Fig. 11, where larger values of $z \propto -\ln\delta\theta$ correspond to smaller angular intervals. Qualitatively, the QCD predictions are confirmed, even though quantitative agreement cannot be claimed. The calculations are rather complicated even in the lowest orders of the perturbation theory and have been only partly pursued to higher orders.

The intermittency indices are directly related to the fractal dimensions of the phase space, defined by the positions of particles inside it.[3] The linear increase in factorial moments in the double-logarithmic scale corresponds to the monofractal structure of the phase space in that region, while their flattening indicates its multifractal structure at lower scales.

3.3.4 Three-jet events. It is possible to single out a subjet with a large transferred momentum at the expense of a small factor α_s in the probability of such a process. One then observes three jets with large angular separation. The Feynman diagram of this process can be obtained from that in Fig. 2 by adding the hard-gluon emission line to a quark (or antiquark). Each of these three partons then evolves to a hadronic jet.

We emphasize the difference between three- and two-jet events. The unique feature of the two-jet events, described by Fig. 2, is the fixed energy of each jet determined by the initial energy. In three-jet events, the emitted gluon takes some energy away from the quark jets, and one has to deal with the energy distribution among the jets. These energies can differ for different selection criteria. Therefore, this provides the possibility to study both soft and hard jets at a given initial energy. Mean multiplicities of particles in a set of jets with energies up to some fixed share of the initial energy of an e^+e^--pair increase with energy according to the same law (8) but with a different factor in front of it, which takes the softer jets in this set into account. We stress that for processes of jet emission in hadronic collisions, one always has to deal with sets of jets with different energies. This is partly because the initial partons are already distributed in energies inside hadrons in accordance with the structure functions.

There exists another important factor that influences the total multiplicity in three-jet events. This is the larger role of interference between jets because of their smaller angular

[3] This is reminiscent of the Cantor set of zero-dimensional points, which has a finite fractal dimension.

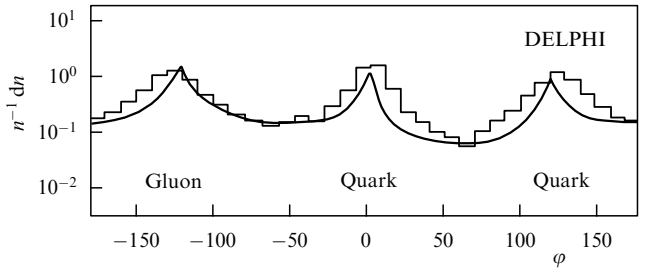

Figure 12. The charged particle flows in three-jet events (hystogram) compared to analytic QCD predictions (solid line) as functions of the jet angles.

separation compared to two-jet events, where the angle between the jet axes is π and the interference can be neglected. It has been shown that multiplicities in three-jet events are also well described by QCD formulas if color coherence, i.e., interference induced by the color contents of the jets, is properly taken into account.

The predicted and observed effects of different suppressions of hadron multiplicities in the regions between the jet axes are very interesting. The QCD color coherence is also responsible for it. The three jets in e^+e^- annihilation processes are different because two of them are formed by the original quark and antiquark and the third is formed by the gluon emitted by one of them. It has been predicted that the number of hadrons emitted in the region between the quark and antiquark should be smaller than in the regions adjoined to the gluon. This suppression is clearly seen in Fig. 12.

Color coherence is also responsible for particle flows in the transverse direction to the reaction plane and for some azimuthal correlations.

3.3.5 Heavy quarks. With some probability, heavy quarks are born in e^+e^- annihilation. [This is taken into account, for instance, in Eqn (6)]. The quark–gluon showers created by them are different from those for light quarks. The emission is suppressed inside the cone in the forward direction, and we can therefore talk about the so-called dead-cone effect or about the ring-like structure of the angular distribution of the emitted partons. In QED, there is an analogous effect because the emission of photons by muons is suppressed compared to electrons due to the larger mass entering the propagator.

Another effect that distinguishes heavy and light quarks is that the gluons emitted by heavy quarks move faster than the heavy quark and quite soon become separated from it, making the color charge screening (analogous to the Chudakov effect for electron–positron pairs in electrodynamics) less important. All this leads to a lower accompanying (i.e., induced by parton showers) multiplicity of heavy quark jets. However, the decay multiplicity of heavy quarks is much higher. Thus, one can predict a positive difference of total multiplicities for heavy and light quarks that is independent of energy. Measurements of the difference between these total multiplicities in e^+e^- annihilation as functions of energy have confirmed the QCD predictions, as demonstrated in Fig. 13. Only this byproduct of the dead-cone effect has been observed, but not the ring-like angular distribution directly, which is strongly shadowed by the decay products.

Another interesting characteristic of heavy quarks is that the hadrons formed by them tend to retain a substantial

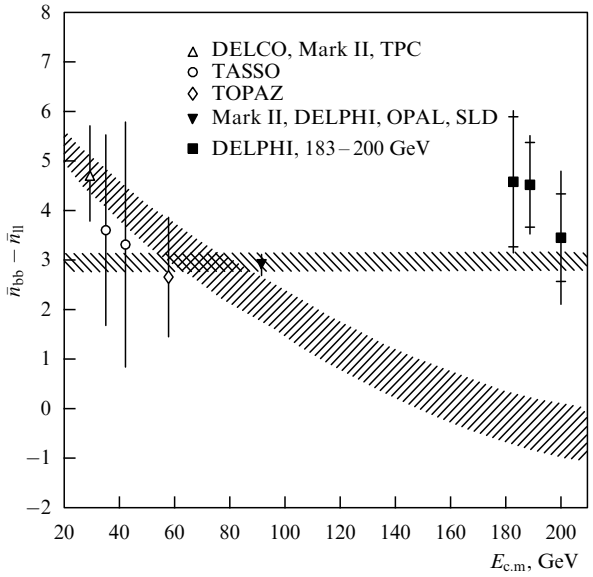

Figure 13. The difference between the mean multiplicities of charged particles in events with b and (u, d, s)-quarks versus the initial energy. QCD predictions (horizontal band) agree with experimental data, while the naive model of simple energy rescaling (decreasing band) does not.

portion of the primary quark energy, thus giving rise to the enhanced leading-particle effect and 'long-flying cascades' in cosmic rays.

3.3.6 Jet universality. QCD prescribes the same properties of jets, independent of the processes in which they were created, because only the parton nature of the object initiating a given jet is of any importance. In Fig. 9, we have already demonstrated the universality of some jet properties in processes with different colliding partners. There are more confirmations of it. However, to describe reactions initiated by hadrons, one should consider their internal structure and introduce some new concepts like structure functions, parton distribution functions, and/or parton fragmentation functions. This is discussed in what follows.

4. Hard processes in deep inelastic scattering and hadronic interactions

4.1 Factorization theorem

In the QCD perturbation theory, it is possible to prove the following factorization theorem for the differential cross section of an arbitrary hard process in collisions of particles a and b:

$$d\sigma_{ab}^{kl} \sim \int dx_i\, dx_j f_a^i(x_i,\mu^2) f_b^j(x_j,\mu^2)\, d\sigma_{ij}^{kl}\,, \qquad (12)$$

where $f_a^i(x_i,\mu^2)$ are distributions of partons i in a hadron a (x_i is the ratio of the longitudinal momentum of the parton i to the momentum of the hadron a and μ is the scale of the hard interaction), and $d\sigma_{ij}^{kl}$ is the differential cross section of the hard subprocess $i+j \to k+l$ that can be calculated in the QCD perturbation theory. The parton distribution functions (pdfs) contain nonperturbative information (x-dependence at some fixed scale μ_0), but their scale dependence can be predicted at large scales using the DGLAP evolution equations.

4.2 Partonic distributions and DIS

One of the main sources of information on pdfs is the process of deep inelastic scattering (DIS) of leptons on nucleons. For neutral currents and virtualities $Q^2 \ll 10^4$ GeV^2, this process is dominated by an exchange of a virtual photon. DIS cross sections are usually described in terms of two structure functions $F_2(x, Q^2)$ and $F_L(x, Q^2)$, where $x = Q^2/(W^2 + Q^2 - m_N^2)$ is the Bjorken variable (W is the invariant mass of the produced hadronic system).

The function $F_2(x, Q^2)$ is related to the total cross section of the virtual photon – proton interaction as

$$\sigma_{\gamma^* \mathrm{p}}^{(\mathrm{tot})}(W^2, Q^2) = \frac{4\pi^2 \alpha_{\mathrm{e.m}}^2}{Q^2} F_2(x, Q^2) . \qquad (13)$$

In the region of large Q^2, the function $F_2(x, Q^2)$ can be expressed in terms of distributions of quarks and antiquarks in hadrons:

$$F_2 = \sum_i e_i^2 x\left[q_i(x, Q^2) + \bar{q}_i(x, Q^2)\right] . \qquad (14)$$

The Bjorken variable x corresponds in the parton model to the relative longitudinal momentum x of a quark (antiquark), introduced above. The function F_2 is measured in a broad range of x, Q^2. The Q^2-dependence of experimental data is in a very good agreement with the DGLAP evolution equations. From these data, it is possible to determine the distributions of quarks and antiquarks in hadrons, and from the Q^2-dependence of the data, one can also determine the distributions of gluons. An example of such an analysis is presented in Fig. 14. We note that the distributions of sea quarks (S) and gluons (g) have an x-dependence strongly different from that of valence quarks. Their densities xS and xg increase strongly as x decreases and reach large values ~ 10 at $x \sim 10^{-3}$. This property is discussed in more detail below.

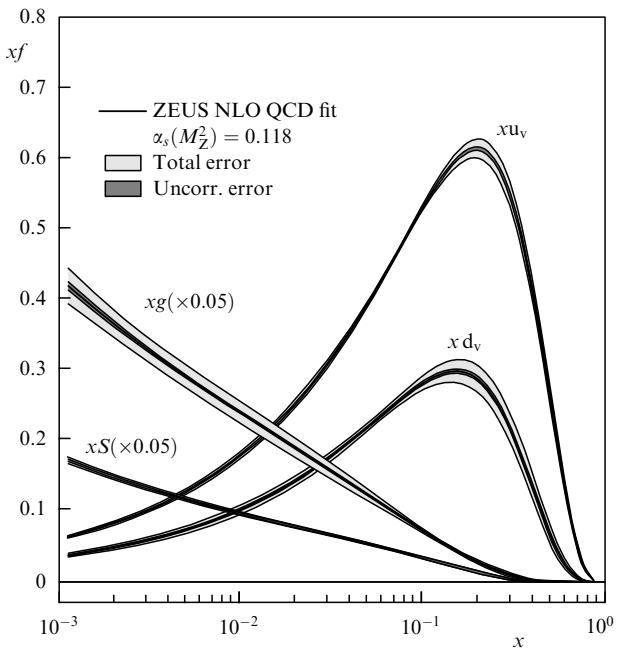

Figure 14. The distributions of gluons (g), sea quarks (S), and valence (u_v, d_v)-quarks extracted by the ZEUS Collaboration from a QCD fit.

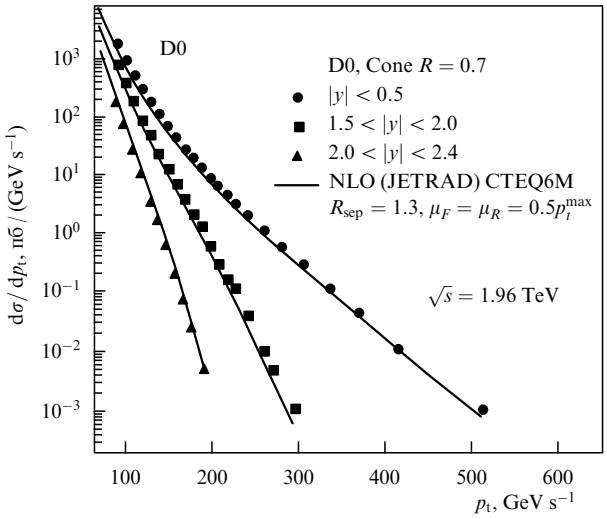

Figure 15. The inclusive jet cross section at Tevatron, measured by the D0 Collaboration as a function of p_t in different rapidity regions.

At present, there are several groups (CTEQ, MRST, and others) performing a global analysis of all experimental data on hard processes. Such an analysis not only provides reliable information on pdfs but also allows testing the self-consistence of perturbative QCD predictions for a broad class of processes.

4.3 Production of jets in hadronic interactions

Hadronic interactions provide the possibility to study a large variety of hard processes: production of hadrons, photons, and jets with large transverse momenta, heavy lepton pairs, heavy quarks, etc. Here, we give one example of these processes: production of jets at Tevatron. New data on this process were obtained recently in the Run II at Tevatron by the *D*0 Collaboration. The differential cross section of jet production as a function of the transverse momentum of a jet is shown in Fig. 15 for different values of rapidity. The curves in this figure correspond to QCD predictions with CTEQ6M pdfs. The agreement between theory and experiment for changing the cross section by many orders of magnitude is impressive. Thus, QCD well describes hard processes in hadronic interactions up to very small distances $\sim 10^{-17}$ cm.

4.4 Small-x physics

It was emphasized above that the structure functions of hadrons increase rapidly as $x \to 0$. Analysis of HERA data shows that for the parameterization of the structure function $F_2(x, Q^2)$ as

$$F_2(x, Q^2) \sim \left(\frac{1}{x}\right)^{\lambda(Q^2)} ,$$

the exponent $\lambda(Q^2)$ increases from a value $\lambda \approx 0.1$ at low Q^2 to values $\lambda \approx 0.4$ at $Q^2 \sim 10^2$ GeV^2. Thus, $\sigma_{\gamma^* \mathrm{p}}^{(\mathrm{tot})}(W^2, Q^2)$ increases with energy at large Q^2 much faster than $\sigma_{\mathrm{pp}}^{(\mathrm{tot})}$. There are good reasons to believe that the rapid increase of $\sigma_{\gamma^* \mathrm{p}}^{(\mathrm{tot})}$ with energy in the HERA energy range will change to a slower increase at much higher energies. Otherwise, there will be problems with the s-channel unitarity in the limit $x \to 0$.

In QCD, the rapid increase of structure functions is related to an increase in the number of partons (especially

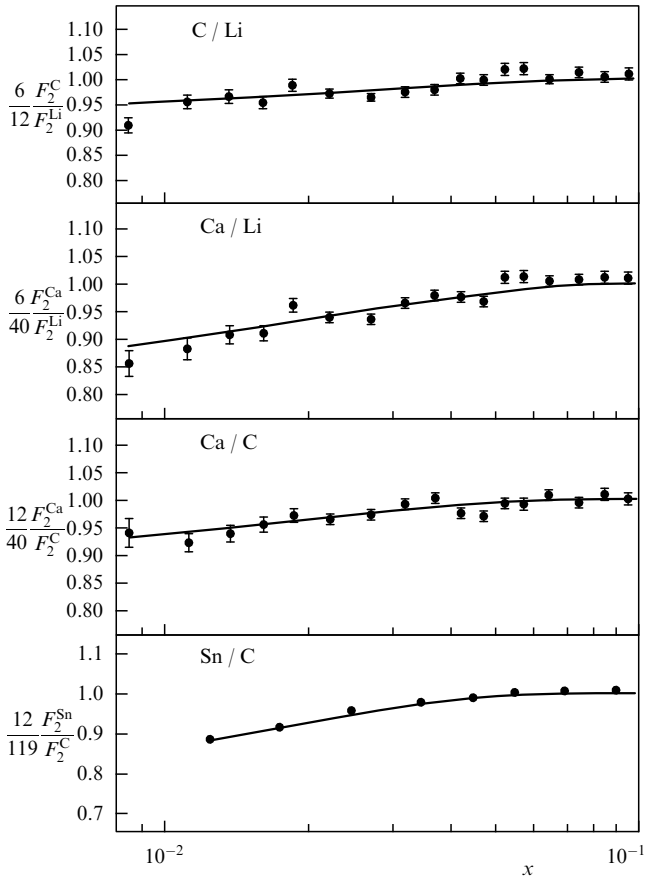

Figure 16. Description of nuclear structure functions in the Glauber–Gribov approach.

gluons) at high energies (as the relative momentum $x \to 0$) due to the quark–gluon cascade. When the system of partons becomes very dense, nonlinear effects due to the fusion of partons become important. They eventually lead to a 'saturation' of parton densities in the limit as $x \to 0$. 'Saturation' extends to higher scales of Q_s^2 as energy increases. There are hopes to calculate these effects in the QCD perturbation theory.

The unitarity effects for distributions of partons are especially important for future hadronic colliders and cosmic rays, because the values of x for interacting partons $x_1 x_2 = M_\perp^2/s$ decrease with energy.

For nuclei, the density of partons at a given impact parameter increases with the atomic number $\sim A^{1/3}$, and therefore nonlinear effects are enhanced. The nuclear shadowing describes the same phenomenon and is clearly seen in the structure functions of nuclei for $x \ll 1/(m_N R_A)$ (Fig. 16). These effects can be calculated using the Gribov–Glauber approach for the scattering of virtual photons on nuclei and information on diffractive dissociation of a virtual photon in γ^*p collisions. Such an approach includes not only perturbative QCD diagrams but also large-distance, nonperturbative dynamics. The results of such calculations are shown by the curves in Fig. 16 and are in good agreement with experimental data.

4.5 Hadroproduction of heavy quarks

As has been described above, QCD radiation by heavy quarks has a specific feature that was predicted theoretically. One could hope that due to the large masses of these quarks, it would be possible to predict their production cross sections with quite good precision. But the situation with QCD calculations is not yet clear, even though there has been great improvement over the last 10–15 years. The total cross sections of the production of particles with open charm and beauty predicted in the 1990s turned out to be small and too slowly increasing with energy compared to recent results of accelerator experiments. Quite large values of these cross sections at high energies were also obtained from the analysis of the long-flying component of extensive air showers and muons in cosmic rays. Recent results taking higher-order (NLO) perturbative corrections into account give larger values and improve the situation, especially at comparatively low energies. But they are still several times lower than experimental data. The quark–gluon string model is in a better position for predicting larger cross sections.

5. Heavy-ion collisions

Investigation of QCD as a function of the temperature T and baryonic chemical potential μ_B can give important information on properties of the theory and possible types of QCD matter. The QCD phase diagram has an interesting structure. At low T and μ_B, one has a matter made of white hadrons, and quarks and gluons are confined. The chiral symmetry of QCD is spontaneously broken. Above some critical curve in the T, μ_B plane, a phase transition to a deconfined system of quarks and gluons occurs and the chiral symmetry is restored. This state is usually called quark–gluon plasma (QGP). At very large μ_B (and small T), there is a color superconductive phase.

Heavy-ion collisions are considered a tool to produce and study a new state of matter: QGP. It is important to theoretically investigate the properties of the quark–gluon system above the critical point of the phase transition. This is usually done using lattice calculations. Some recent calculations show that there can be a strong interaction between quarks and gluons well above the critical point. This makes a formulation of clear signals of QGP formation difficult.

For heavy-ion interactions at very high energies, it is important to know the quark–gluon Fock states of colliding nuclei. It was emphasized above that there are many soft partons with small x in a fast nucleus and there are strong interactions between these partons leading to 'saturation' effects. The quark–gluon state calculated in the QCD perturbation theory in the limit corresponding to 'saturation' was called "the color glass condensate."

These effects lead to a substantial reduction in the densities of hadrons produced in heavy-ion collisions compared to predictions by the model with independent interactions of nucleons (Glauber model). This reduction is already seen at the RHIC energies (see the Table). The theoretical value calculated in the Glauber model takes energy–momentum conservation effects into account, which reduce the density of hadrons produced at not too high energies. The shadowing effects have been calculated in the same model as

Table. Densities of charged hadrons $\mathrm{d}n/\mathrm{d}\eta|_{\eta=0}$ in central Pb–Pb collisions at $\sqrt{s} = 130$ GeV.

Glauber model	With shadowing corrections	Experiment (Phobos)
1200 ± 100	630 ± 120	$555 \pm 12 \pm 35$

the shadowing for nuclear structure functions discussed above.

It is worth noting that the characteristic values of relative longitudinal momenta of partons are $x_i \sim 10^{-2}$ at RHIC and the shadowing of partons is far from 'saturation' in this region of x even for heavy nuclei.

In experiments at RHIC, a decrease in cross sections compared to the number of collisions for production of particles and jets at large $p_\perp$ is also observed. It cannot be attributed to the shadowing of partons (at least in the central rapidity region, because $x_i \sim 0.1$ and shadowing effects are absent in this kinematical region). This effect can be explained as a consequence of final-state interactions (energy loss in a dense medium). It is often considered an indication of QGP. Some recombination processes can also proceed at high parton densities. It is necessary to carry out more detailed theoretical and experimental studies of this problem in order to reach a more definite conclusion on this point.

A jet piercing through the nucleus loses its energy very fast. The multiplicity of produced high-p_t particles becomes lower. This effect has also been observed and was called jet quenching. It has been explained in QCD-based Monte Carlo models, and experimental data have been well fitted.

The typical nuclear effects are clearly seen in the diminishing role of both light hadrons (especially, ρ^0) and quarkonia (the bound states of a heavy quark with its antiquark), and, on the contrary, in the fast increase with energy of the cross sections for heavy quark production.

Collective effects in nuclei are very interesting. Any jet can be regarded as a body moving fast in a medium. It induces some pressure in the nucleus. 'Bounce-off' (the directed flow in the reaction plane) and 'squeeze-out' (the second Fourier moment of the azimuthal particle emission distribution, also called elliptic flow) effects due to this pressure have been observed.

The specific two-maximum angular distributions of particles around the direction of propagation of jets have been measured. They could be produced by Mach waves, which can appear for jets moving with a speed exceeding that of sound in a nucleus considered as a medium. A similar effect can arise due to coherent Cherenkov gluons moving with a phase velocity lower than that of a parton emitting it. The ring-like structure of particle emission in the plane perpendicular to the direction of propagation of jets has been seen. These effects are still waiting for more detailed experimental data and new theoretical approaches to the nonperturbative QCD for an explanation of the collective properties of partons. They should provide us with information about the properties of the quark–gluon matter such as its index of nuclear refraction and speed of sound in it, which are closely related to its equation of state.

6. Conclusion

It is seen from this short review that the QCD perturbation theory is well developed at present and its predictions are in good agreement with a vast amount of data on hard processes in e^+e- ep-, $pp(p\bar{p})$-, pA- and AA-e collisions. QCD has been tested down to very small distances $\sim 10^{-17}$ cm.

At the same time, the problem of color confinement, i.e., the problem of comparatively large distances, has not been solved yet. Its role is usually taken into account by some phenomenological formulas, which describe the parton contents of hadrons and transitions between partonic and hadronic states. Therefore, it is very important to develop a reliable nonperturbative approach to QCD.

References

Monographs.

1. Eden R J *High Energy Collisions of Elementary Particles* (Cambridge: Cambridge Univ. Press, 1967)
2. Okun L B *Leptony i Kvarki* (Leptons and Quarks) (Moscow: Nauka, 1981) [Translated into English (Amsterdam: North-Holland, 1984)]
3. Andreev I V *Khromodinamika i Zhestkie Protsessy pri Vysokikh Energiyakh* (Chromodynamics and Hard Processes at High Energies (Moscow: Nauka, 1981)
4. Huang K *Quarks, Leptons and Gauge Fields* (Singapore: World Scientific, 1982)
5. Ioffe B L, Lipatov L N, Khoze V A *Glubokoneuprugie Protsessy. Fenomenologiya, Kvark-Partonnaya Model'* (Hard Processes. Phenomenology, Quark-Parton Model) (Moscow: Energoatomizdat, 1983); Ioffe B L, Khoze V A, Lipatov L N *Hard Processes* Vol. 1 Phenomenology, Quark-Parton Model (Amsterdam: North-Holland, 1984)
6. Ynduráin F J *Quantum Chromodynamics: an Introduction to the Theory of Quarks and Gluons* (New York: Springer-Verlag, 1983)
7. Okun L B *Fizika Elementarnykh Chastits* (Elementary Particle Physics) (Moscow: Nauka, 1984)
8. Voloshin M B, Ter-Martirosyan K A *Teoriya Kalibrovochnykh Vzaimodeistvii Elementarnykh Chastits* (Theory of Elementary Particle Gauge Interactions) (Moscow: Energoatomizdat, 1984)
9. Dokshitzer Yu L et al. *Basics of Perturbative QCD* (Ed. J Tran Thanh Van) (Gif-sur-Yvette: Editions Frontières, 1991)
10. Kittel W, De Wolf E A *Soft Multihadron Dynamics* (Singapore: World Scientific, 2005)

Review papers

1. Dremin I M, Dunaevskii A M *Phys. Rep.* **18** 159 (1975)
2. Vaĭnsteĭn A I et al. *Usp. Fiz. Nauk* **123** 217 (1977) [*Sov. Phys. Usp.* **20** 796 (1977)]
3. Iliopoulos J "An introduction to gauge theories", Preprint 76-11 (Geneva: CERN, 1976) [Translated into Russian: *Usp. Fiz. Nauk* **123** 565 (1977)]
4. Marciano W, Pagels H *Phys. Rep.* **36** 137 (1978)
5. Kaidalov A B *Phys. Rep.* **50** 157 (1979)
6. Dokshitzer Yu L, Dyakonov D I, Troyan S I *Phys. Rep.* **58** 269 (1980)
7. Reya E *Phys. Rep.* **69** 195 (1981)
8. Mueller A H *Phys. Rep.* **73** 237 (1981)
9. Bander M *Phys. Rep.* **75** 205 (1981)
10. Altarelli G *Phys. Rep.* **81** 1 (1982)
11. Andersson B et al. *Phys. Rep.* **97** 31 (1983)
12. Gribov L V, Levin E M, Ryskin M G *Phys. Rep.* **100** 1 (1983)
13. Bassetto A, Ciafaloni M, Marchesini G *Phys. Rep.* **100** 201 (1983)
14. Frankfurt L, Strikman M *Phys. Rep.* **160** 235 (1988)
15. Levin E M, Ryskin M G *Phys. Rep.* **189** 268 (1990)
16. Dremin I M *Usp. Fiz. Nauk* **164** 785 (1994) [*Phys. Usp.* **37** 715 (1994)]
17. De Wolf E A, Dremin I M, Kittel W *Phys. Rep.* **270** 1 (1996)
18. Khoze V A, Ochs W *Int. J. Mod. Phys. A* **12** 2949 (1997)
19. Lipatov L N *Phys. Rep.* **286** 131 (1997)
20. Wang X-N *Phys. Rep.* **280** 287 (1997)
21. Stirling W J *J. Phys. G: Nucl. Part. Phys.* **26** 471 (2000)
22. Dremin I M, Gary J W *Phys. Rep.* **349** 301 (2001)
23. Khoze V A, Ochs W, Wosiek J, in *At the Frontier of Particle Physics: Handbook of QCD: Boris Ioffe Festschrift* Vol. 2 (Ed. M Shifman) (Singapore: World Scientific, 2001) p. 1101
24. Kiselev V V, Likhoded A K *Usp. Fiz. Nauk* **172** 497 (2002) [*Phys. Usp.* **45** 455 (2002)]
25. Dremin I M *Usp. Fiz. Nauk* **172** 551 (2002) [*Phys. Usp.* **45** 507 (2002)]
26. Kaĭdalov A B *Usp. Fiz. Nauk* **173** 1153 (2003) [*Phys. Usp.* **46** 1121 (2003)]
27. Krasnikov N V, Matveev V A *Usp. Fiz. Nauk* **174** 697 (2004) [*Phys. Usp.* **47** 643 (2004)]
28. Leonidov A V *Usp. Fiz. Nauk* **175** 345 (2005) [*Phys. Usp.* **48** 323 (2005)]